PROCEEDINGS OF THE SIXTH INTERNATIONAL SEMINAR ON
"Recent Research and Design Progress in Aeronautical Engineering and its Influence on Education" – Riga, Latvia

GYROSCOPE-BASED CONTROL AND STABILIZATION OF UNMANNED AERIAL MINI-VEHICLE (MINI-UAV)

R. Chatys, Z. Koruba

Kielce University of Technology (KUT), Al.1000-lecia P.P. 7, 25-314, Poland.
E-mail: chatys@tu.kielce.pl, ksmzko@tu.kielce.pl
Received 18 10 2004, accepted 10 06 2005

Rafał CHATYS was born in 1970 in Kielce (Poland). In 1989 he started a master-level course at the Faculty of Mechanical Engineering, the Riga Institute of Civil Aviation Engineers (RICAE), completing it in 1994. He was awarded a doctor's degree in 1998 by the Chair of the Structure and Strength of Aerial Vehicles, Riga Aviation University (formerly RICAE). Now he works as an assistant professor at the Chair of Metallography and Material Science at the Kielce University of Technology. He is concerned with the problems of mechanics of composite materials and methods for forecasting fatigue properties of polymer composites. He is the author or co-author of over 58 works published in national and foreign professional journals.

Zbigniew KORUBA was born in 1957 inTrzebnica (Poland). In 1982, he graduated from the Kiev Institute of Civil Aviation Engineers (KICAE) with a Master of Mechanical Engineering with honours. He obtained his doctor's degree in 1990 at the Chair of Theoretical Mechanics at KIILC. He was awarded the status of a habilitated doctor in 2001 at the Military Technical Academy in Warsaw. Now he works as a professor at the Chair of Vehicles and Mechanical Equipment at Kielce University of Technology (Poland). He deals with the problems of dynamics, control, and homing of aerial vehicles. He has written more than 80 papers, (30 as a co-author) published in national and foreign professional journals, 1 monograph, and 2 books for university students.

Abstract. This work discusses the use of a mini gyroscope with three degrees of freedom to control or remote control an unmanned aerial mini-vehicle (mini-UAV). The gyroscope determines the reference system for the navigation of the UAV. The algorithm of the gyroscope control moments and the law of deflection of the UAV surface control are presented. The mini autopilot plays a role of a system that makes the longitudinal line coincide with the gyroscope axis. The structure and durability aspects of the remote and programmed navigation are considered.

Keywords: mini-UAV, mini gyroscope, strength, structure of composites.

Introduction

Unmanned aerial mini-vehicles are objects bigger than a human hand that can fly like birds, and have the intelligence of insects. Their field of observation is approximately 10 km, and the unit cost should not exceed US$1,000. In the early 90s, hobbyists only for amusement flew such objects. Soon, however, military organizations became interested in their use, and, for instance, the US Defense Advanced Research Project Agency (DARPA) initiated a four-year project worth $35 million to develop a mini-UAV.

Today, one of the most significant challenges facing aerospace engineering concerned with mini-vehicles is that of improving the drive, flight control, sensors, microelectronics, and micromechanics, and, above all, analyzing the air loads acting on a structure during a controlled flight.

There are various applications of mini-UAVs; though reconnaissance tasks seem to be predominant, they can also be used for passing information to paratroopers. The parameter requirements established for a mini-UAV include: length up to 15 cm, mass 50 g, flight time 30–60 min, flying speed 10–20 m/s, and range 3–10 km. A mini-UAV should be able to provide images at 0.5 ft resolution, reach a target by itself whether in open or closed space, and, in certain versions, also detect chemical, biological, and electronic agents.

There are still a number of problems that flight physicists dealing with flying robots or mini-planes have to explain. Aerospace designers are trying to make the aerodynamics of a mini-UAV resemble the aerodynamics of an insect or a bird as much as possible [6]. Of significance is the relatively high roughness of wings. It makes a bird's surface streamlined for flight or waterproof. In the case of a mini-plane, it not only ensures good aerodynamics but also improves the adherence of the miniaturized instruments and sensors fixed on the wings.

1. New materials for a mini-UAV

To increase the maneuverability of an unmanned aerial vehicle, we can use composites or nanocomposites, the latter being bound to revolutionize 21st century technology [1, 3]. Studying the atomic and molecular structures of materials helps to reconstruct the flight of the bird or an insect. A wing with a fibrous coating improves aerodynamic lift by utilizing vortices and airflow conditioning the complicated flight of a bird.

In the experiment, copper structures made of 3 mm long wire elements were subjected to sintering in accordance with IS 2740 standards [2].

As we know, air enters the body of a bird or an insect through special openings. Then, it is evenly distributed by a system of tracheae. The airflow inside a mini-plane could be forced by the shrinkage and tightening of the composite or nanomaterial particles (material strain). It is essential to reinforce the wing structure, and this can be achieved by applying polymeric fibers, which are to replace radiating levers [4]. An important problem in the flight mechanics of mini-UAVs is to ensure the appropriate stability of motion while realizing programmed trajectories. One of the solutions suggested in such a case seems to be the use of a gyroscope for the automatic flight control of mini-UAV.

2. Gyroscope navigation of a mini-UAV

Consider a mini aerial vehicle with a gyroscope fixed inside or outside it. Assume initially that a symmetrical gyroscope rotor revolves round the *AA* axis having one degree of freedom in relation to the mini-UAV (Fig 1). Since the rotor parts are regularly arranged around the axis of high-speed rotations, the distribution of the mass of the whole mini-UAV-gyroscope system does not change during its operation. Thus, the moments of inertia of the system will be constant and the rotor motion can be described in the same way as that of a single rigid body.

Then, assume that the mini-UAV is a rigid body, i.e. one that does not undergo a deformation, with constant mass. The motion of the mini-UAV-gyroscope system can be represented by means of two systems of equations describing the motion of the system mass center and the motion around the mass center. Additionally, consider the simplest case, when the rotor axis, O_{x_3}, is also the main central axis of inertia of the mini-UAV, Ox.

The equations of translatory motion of the mini-UAV in the related $Oxyz$ coordinate system are given as follows:

$$m_o\left(\frac{d\boldsymbol{u}^*}{dt}+\boldsymbol{w}^*\boldsymbol{q}^*-\boldsymbol{v}^*\boldsymbol{r}^*\right)=\boldsymbol{F}_x \tag{1a}$$

$$m_o\left(\frac{d\boldsymbol{v}^*}{dt}+\boldsymbol{u}^*\boldsymbol{r}^*-\boldsymbol{w}^*\boldsymbol{p}^*\right)=\boldsymbol{F}_y \tag{1b}$$

$$m_o\left(\frac{d\boldsymbol{w}^*}{dt}+\boldsymbol{p}^*\boldsymbol{v}^*-\boldsymbol{q}^*\boldsymbol{u}^*\right)=\boldsymbol{F}_z \tag{1c}$$

where:

m_o – mini-UAV-gyroscope system mass;

$\boldsymbol{u}^*,\boldsymbol{v}^*,\boldsymbol{w}^*$ – components of the linear velocity of the mini-UAV in the related $Oxyz$ coordinate system;

$\boldsymbol{p}^*,\boldsymbol{q}^*,\boldsymbol{r}^*$ – components of the angular velocity of the mini-UAV in the related $Oxyz$ coordinate system;

$\boldsymbol{F}_x,\boldsymbol{F}_y,\boldsymbol{F}_z$ – components of the main vector of external forces acting on the mini-UAV where:

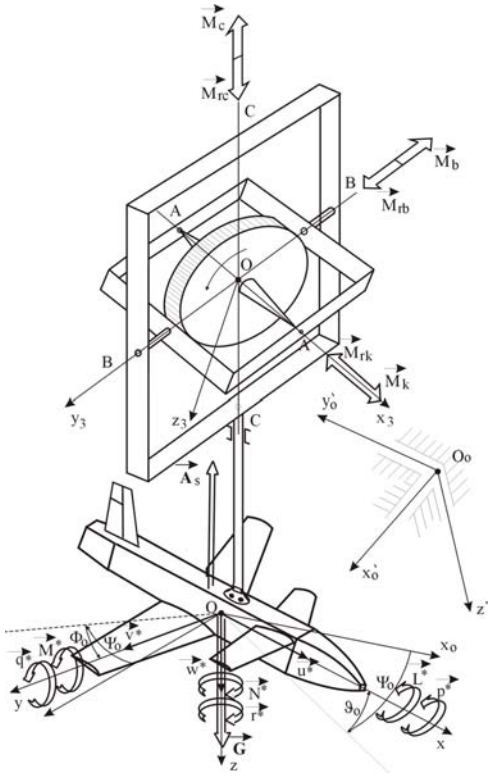

Fig 1. View of the gyroscope control of a mini-UAV with set coordinate systems

$$\begin{bmatrix} \boldsymbol{F}_x \\ \boldsymbol{F}_y \\ \boldsymbol{F}_z \end{bmatrix} = \begin{bmatrix} \boldsymbol{A}_x^s + \boldsymbol{G}_x \\ \boldsymbol{A}_y^s + \boldsymbol{G}_y \\ \boldsymbol{A}_z^s + \boldsymbol{G}_z \end{bmatrix}$$

On the other hand, the equations of rotation of the mini-UAV in the same coordinate system are described as follows:

$$J_{ox}\frac{d\boldsymbol{p}_s}{dt} + \left(J_z - J_y\right)\boldsymbol{q}^*\boldsymbol{r}^* + J_{gx}\frac{d\omega_{gx}}{dt} = \boldsymbol{L}^* \quad (2a)$$

$$J_y\frac{d\boldsymbol{q}^*}{dt} + \left(J_{ox} - J_z\right)\boldsymbol{p}^*\boldsymbol{r}^* + J_{gx}\omega_{gx}\boldsymbol{r}^* = \boldsymbol{M}^* \quad (2b)$$

$$J_y\frac{d\boldsymbol{r}^*}{dt} + \left(J_y - J_x\right)\boldsymbol{p}^*\boldsymbol{q}^* - J_{gx}\omega_{gx}\boldsymbol{r}^* = \boldsymbol{N}^* \quad (2c)$$

where:

J_{ox}, J_{oy}, J_{oy} – main central moments of inertia of the mini-UAV in relation to the particular axes of the $Oxyz$ system;

J_{gx}, J_{gy}, J_{gz} – main central moments of inertia of the gyroscope rotor in relation to the particular axes of the $Oxyz$ system;

ω_{gx} – angular velocity of the high speed rotations of the gyroscope rotor;

$J_y = J_{oy} + J_{gy}$, $J_z = J_{oz} + J_{gz}$;

$\boldsymbol{L}^*, \boldsymbol{M}^*, \boldsymbol{N}^*$ – components of the main vector of the moment of external forces, where:

$$\begin{bmatrix} \boldsymbol{L}^* \\ \boldsymbol{M}^* \\ \boldsymbol{N}^* \end{bmatrix} = \begin{bmatrix} \boldsymbol{L}_A + \boldsymbol{L}_G \\ \boldsymbol{M}_A + \boldsymbol{M}_G + \boldsymbol{M}_b \\ \boldsymbol{N}_A + \boldsymbol{N}_G + \boldsymbol{M}_c \end{bmatrix}$$

$\boldsymbol{L}_A, \boldsymbol{M}_A, \boldsymbol{N}_A$ – components of the main vector of moment of aerodynamic forces;

$\boldsymbol{L}_G, \boldsymbol{M}_G, \boldsymbol{N}_G$ – components of the main vector of moment of the force of gravity;

$\boldsymbol{M}_b, \boldsymbol{M}_c$ – moments of the gyroscope control forces.

3. Kinematics of the coupled motion of the unmanned aerial mini-vehicle (mini-UAV) and the observed ground target (horizontal plane)

The kinematic equations of the mini-UAV motion during the observation and tracing of a ground target moving in the horizontal plane at a set altitude H can be represented in the following form:

$$\frac{dr_h}{dt} = V_c\cos\left(\sigma - \chi_c\right) - V_s\cos\left(\sigma - \chi_s\right) \quad (3a)$$

$$\frac{d\sigma}{dt} = \frac{V_s\sin\left(\sigma - \chi_s\right) - V_c\sin\left(\sigma - \chi_c\right)}{r_h} \quad (3b)$$

$$\frac{d\chi_s}{dt} = \omega_s^*\,\mathrm{sgn}\left(\frac{d\sigma^*}{dt}\right) \quad (3c)$$

where:

r_h – distance between the flight path of the mini-UAV mass center S and that of the target C;

V_s, V_s – flight path velocities of the mini-UAV and the target, respectively;

σ – angle determining the position of the vector $\vec{r}_h$ of location of the mini-UAV in relation to the target in the Oxy plane;

χ_s, χ_c – angles determining the position of the vectors of velocities $\vec{V}_s$ i $\vec{V}_c$ in the Oxy plane, respectively.

If (as in Fig 2)

$$\sigma^* = \sigma - \kappa$$

$$\kappa = \arcsin\frac{r_h^*}{r_h}$$

then

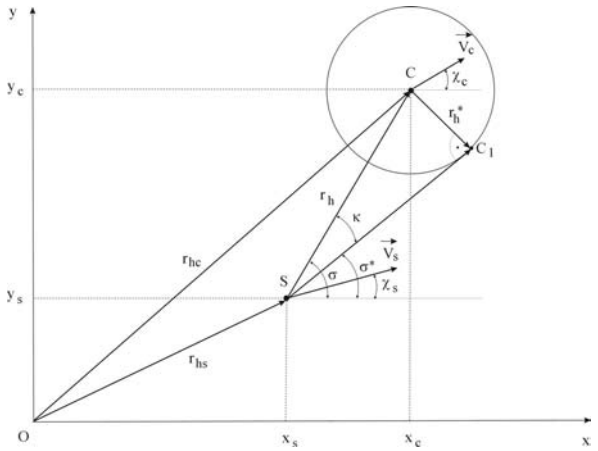

Fig 2. Kinematics of the coupled motion of the mini-UAV and a target in the horizontal plane

$$\frac{d\sigma^*}{dt} = \frac{d\sigma}{dt} + \frac{r_h^*}{\sqrt{\left(r_h\right)^2 - \left(r_h^*\right)^2}\,r_h}\frac{dr_h}{dt} \quad (4)$$

When the distance between the mini-UAV and the target is $r_h = r_h^* = const$, then equation. (3a) will have the form

$$V_c\cos\left(\sigma - \chi_c\right) - V_s\cos\left(\sigma - \chi_s\right) = 0 \quad (5)$$

Thus,

$$\chi_s = \sigma - \arccos\left[\frac{V_c}{V_s}\cos(\sigma - \chi_c)\right] \tag{6}$$

Applying the time-dependent derivative form equation (6), we get:

$$\frac{d\chi_s}{dt} = \frac{d\sigma}{dt} + \frac{\frac{V_c}{V_s}\left[(\dot{\chi}_c - \dot{\sigma})\sin(\sigma - \chi_c) + \left(\frac{\dot{V}_c}{V_c} - \frac{\dot{V}_s}{V_s^2}\right)\cos(\sigma - \chi_c)\right]}{\sqrt{1 - \left[\frac{V_c}{V_s}\cos(\sigma - \chi_c)\right]^2}} \tag{7a}$$

where

$$\frac{d\sigma}{dt} = \frac{V_s \sin\left\{\arccos\left[\frac{V_c}{V_s}\cos(\sigma - \chi_c)\right]\right\}}{r_h^*} - \frac{-V_c \sin(\sigma - \chi_c)}{r_h^*} \tag{7b}$$

If the target is moving with a uniform straight-line motion ($V_c = const$, $\chi_c = const$), and the velocity of the mini-UAV is constant ($V_s = const$), then

$$\frac{d\chi_s}{dt} = \frac{d\sigma}{dt} - \frac{\frac{V_c}{V_s}\sin(\sigma - \chi_c)}{\sqrt{1 - \left[\frac{V_c}{V_s}\cos(\sigma - \chi_c)\right]^2}}\frac{d\sigma}{dt} \tag{7c}$$

In a general case, taking into account (3), (6) and (7), the equations of motion for the mini-UAV in the horizontal plane can be given as follows

$$\frac{dr_h}{dt} = \Pi(t_o, t_w)\cdot\left[V_c\cos(\sigma - \chi_c) - V_s\cos(\sigma - \chi_s)\right] + \Pi(t_w, t_k)\cdot 0 \tag{8a}$$

$$\frac{d\sigma}{dt} = \Pi(t_o, t_w)\cdot\frac{V_s\sin(\sigma - \chi_s) - V_c\sin(\sigma - \chi_c)}{r_h} + \Pi(t_w, t_s)\cdot\frac{V_s\sin(\sigma - \chi_s) - V_c\sin(\sigma - \chi_c)}{r_h^*} \tag{8b}$$

$$\frac{d\chi_s}{dt} = \Pi(t_o, t_w)\cdot\omega_s^*\,\mathrm{sgn}\left(\frac{d\sigma}{dt} + \frac{r_h^*\sqrt{r_h - r_h^*}}{r_h - r_h^*}\frac{dr_h}{dt}\right) + \Pi(t_w, t_k)\cdot\frac{d}{dt}\left\{\sigma - \arccos\left[\frac{V_c}{V_s}\cos(\sigma - \chi_c)\right]\right\} \tag{8c}$$

where:

t_o, t_w, t_s, t_k – process start time, target detection time, target observation time and process finish time, respectively;

$\Pi(\cdot)$ – function of a rectangular pulse.

$\Pi(\cdot)$ If $V_s = const$ i $V_c = 0$

then we have

$$\frac{dr_h}{dt} = -\Pi(t_o, t_w)\cdot V_s\cos(\sigma - \chi_s) + \Pi(t_w, t_k)\cdot 0 \tag{9a}$$

$$\frac{d\sigma}{dt} = \left[\Pi(t_o, t_w)\cdot\frac{1}{r_h} + \Pi(t_w, t_k)\cdot\frac{1}{r_h^*}\right]\cdot V_s \tag{9b}$$

$$\frac{d\chi_s}{dt} = \Pi(t_o, t_w)\cdot\omega_s^*\,\mathrm{sgn}\left(\frac{d\sigma}{dt} + \frac{r_h^*\sqrt{r_h - r_h^*}}{r_h - r_h^*}\frac{dr_h}{dt}\right) + \Pi(t_w, t_k)\cdot\frac{d}{dt}\left(\sigma - \frac{\pi}{2}\right) \tag{9c}$$

The trajectory of the mini-UAV motion

$$\frac{dx_s}{dt} = V_s\cos\chi_s \tag{10a}$$

$$\frac{dy_s}{dt} = V_s\sin\chi_s \tag{10b}$$

$$\frac{dz_s}{dt} = 0 \tag{10c}$$

The trajectory of the target motion

$$\frac{dx_c}{dt} = V_c\cos\chi_c \tag{11a}$$

$$\frac{dy_c}{dt} = V_c\sin\chi_c \tag{11b}$$

$$\frac{dz_c}{dt} = 0 \tag{11c}$$

4. Gyroscope Control

There are three methods of gyroscope-based control: a) autonomous, b) remote and c) combined. The first method assumes that the gyroscope realizes a set motion program. The course of the UAV is maintained by the autopilot in such a way that the UAV longitudinal axis coincides with the gyroscope axis. The angles determining the position of the gyroscope axis, ϑ_g and ψ_g, should be equal to the angles determining the position of the UAV longitudinal axis, ϑ_o and ψ_o:

$$\vartheta_o = \vartheta_g, \quad \psi_o = \psi_g. \tag{12}$$

This allows the UAV to reach a desired point in space along a set trajectory. The procedure can be used in the navigation of unmanned aerial vehicles. However, sometimes the autopilot does not take into account the gyroscope motions while realizing a predetermined motion. The gyroscope axis has the motion programmed; it rolls, for instance, to describe an enhanced area of a circular or elliptical cone, i.e. it moves along the spiral of Archimedes. As soon as the gyroscope axis assumes a desired position in space, which may coincide with the moment of target detection, the gyroscope starts operating in the trace-the-target mode and the UAV autopilot employs the established algorithm of control. As a result, the UAV circulates over a detected target or approaches it using the signals about the gyroscope position, as is the case of homing missiles or guided bombs.

The second method involves controlling the gyroscope from a distance. An operator at the command-and-control point observes through a camera the area above, which the UAV flies. The moment the target is detected, the operator positions the sight that is the gyroscope axis. From now on, the UAV (e.g. a guided bomb, armor piercing shell, etc.) will move towards the target.

The third, combined, method of gyroscope-based control can be used in combat unmanned aerial vehicles. First, the UAV is programmed to reach the area of a target location. Then, the gyroscope switches into the target-tracking mode, which involves scanning the space by the gyroscope axis. Finally, after the target is detected, the axis moves in accordance with the displacement of the target observation line, i.e. a straight line connecting some selected points of the UAV and the target.

Whichever control method is applied, the control moments can be represented in the following form [6]

$$\begin{aligned} M_b &= M_b^p + M_b^k \\ M_c &= M_c^p + M_c^k \end{aligned} \tag{13}$$

In equations (11), the quantities M_b^p and M_c^p stand for program controls, which are determined from the inverse problem of dynamics [6, 7]:

$$M_b^p(t) = \mathbf{\Pi}(t_0, t_w) \cdot \cdot \left[\ddot{\vartheta}_{gz} + b_b \dot{\vartheta}_{gz} - \frac{1}{2}(\dot{\psi}_{gz})^2 \sin 2\vartheta_{gz} - \dot{\psi}_{gz} \cos \vartheta_{gz} \right] \cdot \frac{1}{J_g} \tag{14a}$$

$$M_c^p(t) = \mathbf{\Pi}(t_0, t_w) \cdot [\ddot{\psi}_{gz} \cos^2 \vartheta_{gz}^p + b_c \dot{\psi}_{gz} + \\ + \dot{\psi}_{gz} \dot{\vartheta}_{gz} \sin 2\vartheta_{gz} + \dot{\vartheta}_{gz} \cos \vartheta_{gz}] \cdot \frac{1}{J_g} \tag{14b}$$

where: $\Pi(\cdot)$ – functions of a rectangular pulse; t_o – commencing the tracking process, t_w – target location time; J_g – lateral moment of inertia of the gyroscope rotor, $\vartheta_{gz}, \psi_{gz}$ – set angles determining the position of the gyroscope axis in space.

$$M_b^s(t) = \Pi(t_s, t_k) \cdot \left(k_b \cdot e_\vartheta - k_c \cdot e_\psi + h_g \frac{de_\vartheta}{dt} \right) \tag{15a}$$

$$M_c^s(t) = \mathbf{\Pi}(t_s, t_k) \cdot \left(k_b \cdot e_\psi + k_c \cdot e_\vartheta + h_g \frac{de_\psi}{dt} \right) \tag{15b}$$

where: $e_\vartheta = \vartheta_g - \vartheta_c$, $e_\psi = \psi_g - \psi_c$; ϑ_c, ψ_c – angles determining the position of the target observation line; t_s – commencing the tracking process; t_k – end of the tracking process; k_b, k_c – coefficients of the regulator amplification; h_g – coefficient of the regulator damping.

In the programmed control of the gyroscope axis, it is necessary to set the following angular velocities and accelerations:

$$\frac{d\vartheta_{gz}}{dt} = 0, \quad \frac{d^2\vartheta_{gz}}{dt^2} = 0, \tag{16a}$$

$$\frac{d\psi_{gz}}{dt} = \frac{d\sigma}{dt}, \quad \frac{d^2\psi_{gz}}{dt^2} = \frac{d^2\sigma}{dt^2}. \tag{16b}$$

The quantity $\frac{d\sigma}{dt}$ is determined from equation (9b),

while $\frac{d^2\sigma}{dt^2}$ is equal to

$$\frac{d^2\sigma}{dt^2} = \frac{1}{r_h^*} \left\{ \dot{V}_s \sqrt{1 - \frac{V_c^2}{V_s^2} \cos^2(\sigma - \chi_c)} + \right. \\ \left. + \frac{V_c}{V_s} \frac{1}{\sqrt{1 - \frac{V_c^2}{V_s^2} \cos^2(\sigma - \chi_c)}} \times \right.$$

$$\times\left[\frac{1}{V_s}\cos^2(\sigma-\chi_c)\left(\dot{V}_s V_c-\dot{V}_c V_s\right)+\right.$$

$$\left.+\frac{1}{2}V_c\sin 2(\sigma-\chi_c)\cdot(\dot{\sigma}-\dot{\chi}_c)\right]+ \quad (16c)$$

$$\left.+\dot{V}_c\sin(\sigma-\chi_c)+V_c\cos(\sigma-\chi_c)\cdot(\dot{\sigma}-\dot{\chi}_c)\right\}$$

If $V_s = const$ and $V_c = const$, and the target is being approached according to proportional navigation, we get

$$\frac{d^2\sigma}{dt^2}=-\frac{\dot{r}_h}{r_h^2}\left[V_s\sin(\sigma-\chi_s)+V_c\sin(\sigma-\chi_c)\right] \quad (17)$$

and, while tracing and lightening the target, we get

$$\frac{d^2\sigma}{dt^2}=\frac{V_c}{V_s r_h^*}\frac{1}{\sqrt{1-\frac{V_c^2}{V_s^2}\cos^2(\sigma-\chi_c)}} \quad (18)$$

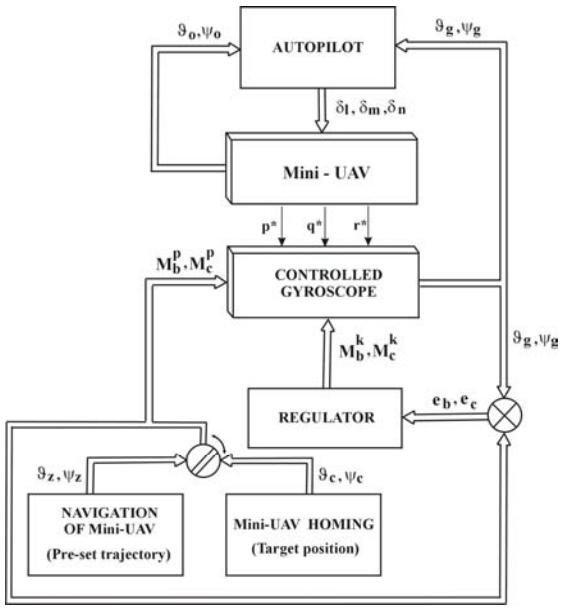

Fig 3. Gyroscope control of a mini-UAV

Additionally, if the target is immovable ($V_c = 0$), and the target is being approached, we have

$$\frac{d^2\sigma}{dt^2}=-\frac{\dot{r}_h}{r_h^2}V_s\sin(\sigma-\chi_s) \quad (19)$$

and, while tracing the target, it is

$$\frac{d^2\sigma}{dt^2}=0 \quad (20)$$

The law of control established by the autopilot (i.e. the height and direction rudder angles, δ_m and δ_n respectively) of the mini-UAV is as follows:

$$\delta_m(t)=k_m\left(\vartheta_g-\vartheta_o\right)+h_m\left(\dot{\vartheta}_g-\dot{\vartheta}_o\right) \quad (21a)$$

$$\delta_n(t)=k_n\left(\psi_g-\psi_o\right)+h_n\left(\dot{\psi}_g-\dot{\psi}_o\right) \quad (21b)$$

where:

k_m, k_n – coefficients of autopilot amplification;

k_m, k_n h_m, h_n – coefficients of autopilot damping.

Figure 3 illustrates a schematic diagram of the navigation of a flying object using a controlled gyroscope.

Conclusion

Advances in the design of nanomachines and nanorobots are possible thanks to the use of nanomaterials and nanocomposites. Knowledge of the new materials enables us to make the flight of a mini-UAV and the flight of a bird or an insect exactly alike.

The results of the research on the application of a gyroscope as the executive element of the mini-UAV automatic control system confirm that it is possible to improve the stability and controlability of the apparatus [7].

It should be noted that the parameters of the gyroscope and the UAV autopilot regulator have to be selected in an optimal way due to the minimum time of transient process fading, which results from external interference or switching on the control system of the gyroscope (control loop 1) and the flying object (control loop 2). Otherwise, the aerial vehicle will not move along the predetermined trajectory, and the intercepted target may disappear from the narrow visual field of the tracking system lens.

References

1. **Pietrucha J., Sibilski K.** Od stworzeń latających do miniaturowych statków powietrznych // Nauka, innowacje, technika. – 2003. – No 1. – P.12–18.
2. **Brusow W., Tiumentsev Yu.** Advanced information technologies and their application in the aeronautics // Proceedings of the second Seminar on Recent research and design progress in aeronautical engineering and its influence on education. – Warsaw, 1996. – P. 93–97.
3. **Chatys R., Orzechowski T.** The diffusion sintering of metallic composites in the construction of highly efficient heat exchangers // Computer – Aided Systems for Manufacture and Measurement of Machine Elements. – CEEPUS, 2003. – P. 61–72.
4. **Chatys R.** Adhesion Strength Estimation between Different Composite Components // Journal of Transport and Engineering. Transport: Aviation transport. – 2003. –Vol 6, No 11. – P. 6–11.

5. **Koruba Z.** Dynamics and Control of a Gyroscope on the Board of an Aerial Vehicle // Monographs, Studies, Dissertations. – Kielce: Kielce University of Technology, 2001. – No 25. – P. 285.

6. **Koruba Z.** Selection of the optimum parameters of the gyroscope system on elastic suspension in the homing missile system // Journal of Technical Physics / Polish Academy of Sciences, Institute of Fundamental Technological Research, Warsaw Military University of Technology. – Warsaw, 1999. – Vol 40, No 3. – P. 341–354.

7. **Каргу Л.И.** Гироскопические приборы и системы // Судостроение. – Ленинград, 1988.